

Z. Malanchuk*¹,
orcid.org/0000-0001-8024-1290,
V. Moshynskiy¹,
orcid.org/0000-0002-1661-6809,
V. Lozynskiy²,
orcid.org/0000-0002-9657-0635,
Ye. Malanchuk¹,
orcid.org/0000-0001-9352-4548,
V. Korniienko³,
orcid.org/0009-0007-5226-4752

1 – National University of Water and Environmental Engineering, Rivne, Ukraine

2 – Dnipro University of Technology, Dnipro, Ukraine

3 – University of Comenius, Bratislava, Slovak Republic

* Corresponding author e-mail: malanchykr@ukr.net

MODELING OF BASALT TUFF BENEFICIATION BY DRY HIGH-INTENSITY MAGNETIC SEPARATION

Purpose. To identify the regularities governing the influence of magnetic field induction and particle size distribution on the technological performance of dry high-intensity magnetic separation (DHIMS) of tuff raw materials and on the quality of the resulting magnetic product.

Methodology. The study was carried out using a laboratory-scale dry magnetic separation unit. The behavior of tuff was investigated in narrow particle-size fractions of +0.63–2.5 and +0.1–0.63 mm under varying magnetic field induction (0–1.3 T), while maintaining constant separator design parameters and a fixed material feed regime. Technological performance was evaluated based on yields of magnetic and non-magnetic fractions, the calculation of distribution functions, and the construction of regression models. The chemical composition of the products was determined by X-ray fluorescence (XRF) analysis.

Findings. The tuff was found to exhibit enhanced magnetic susceptibility and high friability, creating favorable conditions for efficient dry magnetic separation. The average yield of the magnetic fraction for the two samples studied was 51.8 %, with more than 98 % recovery achieved at magnetic field induction values up to $B = 0.58$ T. The regression models show a high degree of correlation ($P_z = 0.97–0.975$) within the acceptable induction range up to $B \approx 0.9$ T. XRF analysis of the magnetic product revealed an Fe_2O_3 content of 30.89 %, confirming effective concentration of iron-bearing components in the magnetic fraction.

Originality. Mathematical modeling of the DHIMS process for tuff was performed for narrow particle-size classes, with the distribution function of magnetic separation product yield determined as a function of magnetic field induction. A consistent pattern of dependencies was established for the investigated size classes, and the statistical significance of the regression model parameters was confirmed (significance level ≤ 0.05). It was demonstrated that linear-logarithmic models provide the best description of the process up to an induction of 0.9 T.

Practical value. The results enable a substantiated selection of DHIMS operating regimes for the integrated processing of tuffs, identification of rational particle-size classes for the removal of magnetic impurities, and prediction of process efficiency based on magnetic field induction. The obtained regression relationships can be applied in the design and optimization of preliminary beneficiation schemes for tuff raw materials, aimed at reducing the mass of material fed to subsequent energy-intensive operations.

Keywords: *tuff, dry magnetic separation, magnetic field induction, particle size distribution, iron-bearing minerals, magnetic fraction*

Introduction. Tuffs are an important target for processing in the mining and construction industries, as these volcanogenic rocks often contain valuable components, particularly zeolites and feldspars. At the same time, their mineralogical composition is multicomponent, which creates substantial technological challenges

for beneficiation and further utilization. To meet quality standards, especially in the production of high-purity ceramics and glass, the targeted removal of harmful impurities is required [1, 2]. In the context of Ukraine's post-war reconstruction, the role of non-metallic minerals as a raw material base for the construction and infrastructure sectors is becoming increasingly important [3].

Tuff raw materials are considered promising for construction and thermal insulation applications, provided

that the required quality and stability of the properties can be ensured [4, 5]. The key impurities to be removed from tuffs are weakly magnetic iron oxides and hydroxides, including hematite, limonite, and related phases [6]. The presence of these paramagnetic impurities in a finely dispersed state makes dry high-intensity magnetic separation (DHIMS) a viable option as a core operation in an integrated tuff processing flowsheet [7]. At the same time, the efficiency of DHIMS strongly depends on ore-preparation parameters, primarily particle size distribution, as well as on the separator's design and operating characteristics.

The integrated processing of tuff raw materials is consistent with the principles of a transition toward resource-efficient, environmentally oriented technologies [8].

Against this background, technological approaches to tuff beneficiation are of both scientific and practical importance for expanding the resource base of non-metallic mineral raw materials. In particular, special attention should be given to selecting rational ore-preparation conditions and separation parameters that ensure efficient removal of iron-bearing impurities while preserving the useful silicate and zeolitic components of the material. This determines the relevance of further analysis of previous studies devoted to the composition of tuffs, their comminution behavior, and the application of dry magnetic separation in integrated processing flowsheets.

Literature review. During ore preparation and the sampling of tuff from basalt quarry dumps and boreholes, it is necessary to investigate its particle-size distribution to properly select equipment and define subsequent processing stages [4]. The established strengthening effect of tuff under repeated water irrigation requires a more precise characterization of its granulometric condition, both within the dump mass and after crushing and grinding. The growing interest in tuff extraction is associated with the expansion of its fields of application, including agriculture, construction, and medicine, which underscores the need to improve processing methods and upgrade the material into a final product that meets the requirements of a specific end use. The rich mineralogical composition of tuffs and their elevated contents of iron and titanium, as well as native copper in the tuffs of Volyn, necessitate their integrated processing [9, 10], the initial stage of which is the preparation of the rock mass for the recovery of valuable components [6, 11].

Two methods of tuff extraction are considered: borehole hydraulic mining and open-pit quarrying [12]. The coarsest tuff material is obtained during basalt quarrying, where bench blasting produces tuff that, being less competent than basalt and lava breccia, is characterized by a finer degree of fragmentation. To substantiate the technology for further processing, it is therefore necessary to study the particle size distribution of tuff both in the dump and during crushing [13].

Practical results of tuff processing confirm the technological feasibility of using magnetic separation as part of the overall integrated processing flowsheet [11]. The purpose of this process is not only to remove impurities, but also to achieve preliminary concentration of the valuable mineral and reduce the mass of material fed to subsequent, often more expensive, beneficiation stages.

The application of dry high-intensity magnetic separation (DHIMS) enables high-efficiency operation; in particular, the yield of enriched tuff may reach 54 %.

The fundamental principle of DHIMS is the generation of a strong magnetic field, either electromagnetic or permanent, in which material particles are subjected to magnetic forces that enable separation based on differences in magnetic susceptibility between the target material and impurities. For the beneficiation of weakly magnetic ores, including tuffs, the most suitable separators are those capable of producing a high magnetic field gradient, which increases the probability of recovering weakly magnetic impurities [14]. In dry beneficiation practice, magnetic roll separators and induction roll/rotor systems are widely used, as their designs ensure continuous removal of attracted grains from the high-field zone and discharge into the magnetic product. At the same time, other separator types, such as column separators, which are primarily intended for the recovery of ferromagnetic impurities, are less effective for extracting weakly magnetic impurities from finely dispersed tuffs.

Along with the technological advantages of DHIMS, the application of induction roll and rotor separators requires consideration of energy and economic aspects. A substantial share of the consumed power is spent not on generating the magnetic field itself, but on mechanical needs, primarily roll rotation, which ensures process continuity; according to reported estimates, this share may reach 60–70 %. Therefore, in addition to magnetic parameters, engineering parameters of feed preparation, and, above all, particle size, are critical. The recovery of weakly magnetic impurities requires sufficient liberation of mineral grains, and the process's optimization criteria are interdependent, since low magnetic susceptibility may be compensated by increasing the magnetic field induction and selecting an appropriate particle size range. At the same time, in most available studies, DHIMS parameters are considered only fragmentarily, without a quantitative generalization of the effects of magnetic field induction and particle size.

Unsolved aspects of the problem. Despite the proven practical efficiency of dry high-intensity magnetic separation (DHIMS), the issue of quantitatively substantiating process parameters for tuff raw materials remains relevant, particularly regarding their particle size characteristics and the degree of mineral grain liberation. One of the key factors determining the efficiency of dry magnetic separation is particle size, since the recovery of weakly magnetic impurities requires nearly complete grain liberation so that the magnetic forces act predominantly on the target particles. The removal of paramagnetic impurities requires a high-intensity magnetic field, and the recovery efficiency increases with increasing magnetic field induction, which justifies the use of high-intensity separation equipment.

At the same time, the optimization criteria of DHIMS are interdependent: the relatively low magnetic susceptibility of certain impurities can be compensated for by increasing the magnetic field induction, selecting an appropriate particle size range, and adjusting engineering parameters related to feed delivery. Under such conditions, a mathematical description of the process [15], particularly in the form of distribution functions and regression models, is required to generalize experi-

mental data and improve the validity of selecting DHIMS operating conditions for different narrow particle size classes, while also providing a basis for predicting technological performance indicators [16].

Purpose of the article and research objectives. The purpose of this study is to establish the regularities of the influence of magnetic field induction and particle size distribution during dry high-intensity magnetic separation (DHIMS) on the efficiency of recovering the magnetic-bearing fraction of tuff raw material and on the quality of the obtained product.

To achieve this purpose, the following objectives were set:

- to investigate the particle size distribution of tuff, both quarry-extracted and obtained by borehole hydraulic mining, taking into account the weakening effect;
- to assess the performance indicators of dry magnetic separation for narrow size classes under different values of magnetic field induction;
- to calculate distribution functions and develop regression models describing the dependence of the yield/recovery of the magnetic product on field induction;
- to confirm the quality of the magnetic fraction based on chemical analysis data and to substantiate the feasibility of applying DHIMS in integrated tuff processing flowsheets.

The results obtained may provide a scientific basis for further R&D in integrated processing of mineral raw materials [17].

Methods. Research material and sample preparation. Dry magnetic separation has specific features in both comminution and classification processes and in the recovery of valuable components, which necessitate consideration of magnetic separator characteristics and the quality of material preparation [18]. A typical technological flowsheet for preparing tuffs for further use or beneficiation integrates dry separation into a closed circuit with mechanical processing operations [11].

The initial material preparation stage included crushing and grinding. Since DHIMS requires feed material within a specified size range, dry magnetic separation was carried out in a closed circuit with crushing and screening: material that did not meet the particle size requirements was returned for further size reduction [19].

Basaltic tuff from the quarry of PJSC “Rafalivskiy Quarry” (Rivne region, Ukraine) was used for the study. The research was conducted jointly with scientists from the Institute of Geotechnical Mechanics of the NAS of Ukraine (Dnipro) and the National University of Water and Environmental Engineering.

Particle size analysis was performed on zeolite-smectite tuffs from the Rafalivskiy basalt quarry by screening 1 m³ of dumped tuff mass on a vibrating screen before and after crushing. Undisintegrated tuff and tuff subjected to several cycles of water irrigation were studied separately to assess the effect of disintegration on the particle size condition of the material. After sample preparation and particle size characterization, the study proceeded to laboratory-scale dry magnetic separation experiments to evaluate the separation behavior of tuff under controlled operating conditions. For this purpose, a dedicated experimental setup was used, the design and operating principle of which are described below.

Experimental setup and operating principle. The general view of the laboratory setup used for dry magnetic separation is shown in Fig. 1.

The setup comprises a feed unit 2–4, a magnetic drum 5 with a drive 6, a flow separation unit with an adjustable splitter 7, 8, and receiving chutes for the magnetic and non-magnetic fractions 9, 10. Material from the hopper passes through the adjustable gate opening to the vibrating feeder, then is delivered as a uniform layer onto the drum shell’s working surface. Under the action of the magnetic field, magnetically susceptible components are retained on the drum surface, conveyed through the field zone, and, after leaving it, separated and directed to the magnetic fraction collector. The non-magnetic portion of the material follows its natural trajectory and is discharged into the non-magnetic fraction collector. A protective cover is provided to prevent material from being ejected from the working area.

During the experiments, the structural parameters of the separator and the material feed conditions were kept constant, while the magnetic field induction was used as the controlled variable. The laboratory investigations were carried out in compliance with occupational safety requirements and working environment conditions [20, 21].

Measurements and analytical methods. The separator’s performance was evaluated based on the magnetic field induction at the drum shell’s surface. The magnetic field induction was varied from 0 to 1.3 T. It was monitored using a teslameter, in accordance with the instrument manual, by measuring the maximum radial component of magnetic induction along the circumference of the drum shell.

For the qualitative and quantitative elemental analysis of magnetic separation products, an Expert 3L X-ray fluorescence rapid analyzer was used, which made it possible to determine the elemental composition of the magnetic fraction and to evaluate the concentration of iron-bearing and associated components in the obtained product.

Data processing and modeling. The technological performance of dry magnetic separation was evaluated

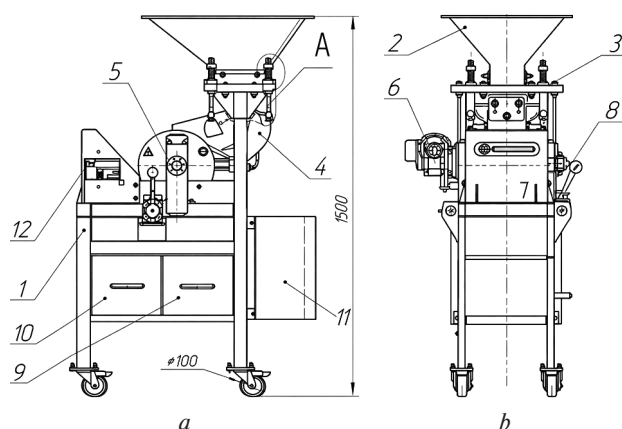


Fig. 1. Laboratory setup for dry magnetic separation:

- a – side view; b – front view: 1 – frame (wheel-mounted base); 2 – feed hopper; 3 – gate; 4 – vibrating feeder; 5 – magnetic drum (shell); 6 – drum drive gear motor; 7 – flow splitter; 8 – splitter position adjustment mechanism; 9 – chute for the magnetic fraction; 10 – chute for the non-magnetic fraction; 11 – control panel; 12 – protective cover

based on the yields of the magnetic and non-magnetic fractions in selected narrow particle size classes. The efficiency of DHIMS was investigated for the +0.63–2.5 and +0.1–0.63 mm size classes at different values of magnetic field induction.

To generalize the experimental data, cumulative distribution functions of the magnetic product were calculated, where the distribution function q_i was defined as the ratio of the magnetic product yield at a given induction to the total magnetic product yield in the sample [22].

To quantitatively describe the process regularities, regression models were developed to describe the dependence of technological indicators, namely the yield/recovery of the magnetic fraction, on magnetic field induction across different narrow particle size classes [15]. Model adequacy was assessed using correlation indicators and statistical significance criteria for the regression coefficients [23] at a confidence level of 0.95.

Results and discussion. The particle size distribution and lithological composition of rocks significantly influence the course of subsequent processing operations [24]. The study established that the largest fragments in the undisintegrated dumped tuff mass are 250–300 mm in size, accounting for 2–3 % of the total. After disintegration, the maximum fragment size decreases to 100–150 mm, while their proportion does not exceed 5 %. These data confirm the substantial effect of disintegration caused by cyclic water irrigation on the particle size condition of the tuff mass and its suitability for subsequent crushing operations.

The particle-size distribution of tuff after borehole hydraulic mining differs significantly from that of quarry tuff and exhibits distinct characteristics depending on the degree of disintegration. Fig. 2 presents the particle size distribution, Q (mm), for quarry tuff before 1 and after 2 disintegration, while Fig. 3 shows the corresponding relationships for tuff obtained by borehole hydraulic mining. In the latter case, the particle size distribution was determined experimentally for 1 m³ of tuff deposited on the hydraulic fill map.

For the quantitative description of the obtained relationships, an analytical distribution model in the form of a power-law dependence was used

$$Q = ax^b,$$

where a , b are model coefficients; Q is particle size, mm; x is cumulative yield, %.

The approximation results confirm that, for quarry tuff both before and after disintegration, the power-law model adequately describes the particle size distribution (Fig. 2). At the same time, for the disintegrated material, a change in the model parameters is observed, reflecting a redistribution of mass toward finer fractions. For tuff obtained by borehole hydraulic mining (Fig. 3), the approximation is also satisfactory. However, the R^2 values are lower than those for quarry material, consistent with the greater variability in particle size distribution and the influence of hydraulic deposition conditions.

Based on the results, a roll crusher with an adjustable gap between the rolls was recommended for further crushing, and the crushability of the initial undisintegrated and disintegrated tuff was also investigated.

To substantiate further ore preparation and the selection of the crushing equipment type, the crushability

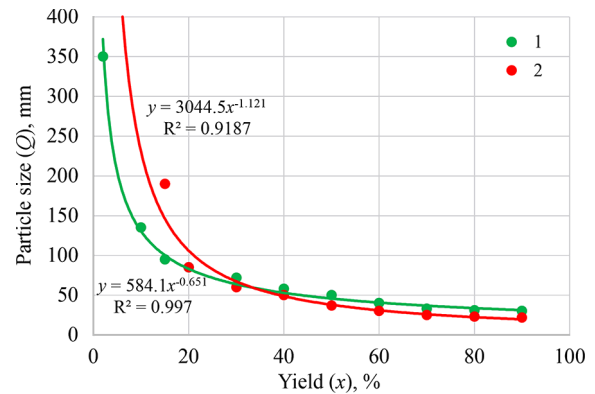


Fig. 2. Particle size distribution of quarry tuff before (1) and after (2) disintegration (recalculated per 1 m³ of rock mass)

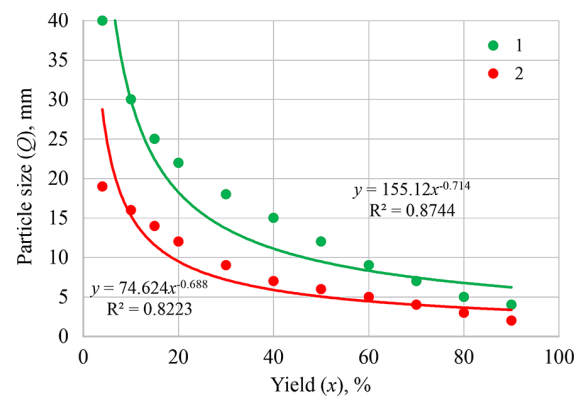


Fig. 3. Particle size distribution of tuff obtained by borehole hydraulic mining before (1) and after (2) disintegration (recalculated per 1 m³ of rock mass)

of the initial undisintegrated and disintegrated tuff was studied using a roll crusher with a variable gap between the rolls. Fig. 4 shows the relationships between the particle size of crushed undisintegrated tuff γ (mm) and yield x (%) at roll gap settings in the range of $\Delta = 3$ –10 mm. Fig. 5 presents analogous results for disintegrated tuff under the same roll gap adjustment conditions.

The analysis of the obtained relationships shows that variation in the roll gap significantly affects the particle size distribution of the crushing product: a decrease in Δ results in a finer product while maintaining a stable yield distribution. Fine fractions generated at the crushing stage may be regarded as a potential secondary mineral raw material for further technological applications [25].

The agreement between the experimental data and the theoretical curves (Figs. 4, 5) confirms the use of a power-law model to describe the particle-size distribution of the crushed material. For the quantitative description of these relationships, an analytical model in the form of a power function was used

$$\gamma = ax^b,$$

where a , b are model coefficients; γ is the particle size of crushed tuff, mm; x is cumulative yield, %

The obtained results, together with the particle-size analysis data for quarry and hydraulically mined borehole material, allow the conclusion that roll crushing is an expedient principal solution at the ore-preparation stage. In particular, the feasibility of further tuff size re-

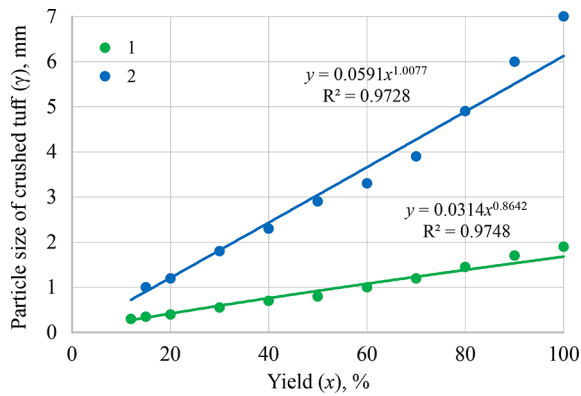


Fig. 4. Dependence of the particle size of crushed undisintegrated tuff on yield x (%) at different gaps between the rolls of the roll crusher:

1 – $\Delta = 3$ mm; 2 – $\Delta = 10$ mm

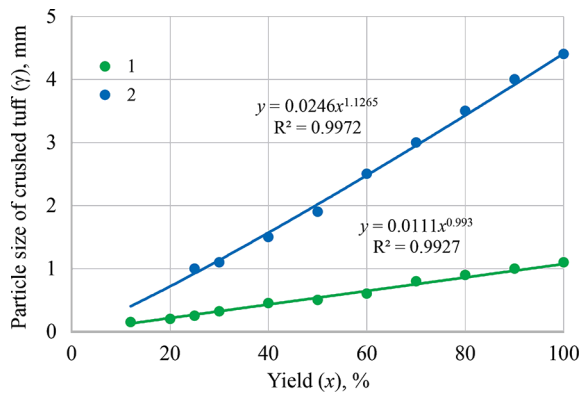


Fig. 5. Dependence of the particle size of crushed disintegrated tuff on yield x (%) at different gaps between the rolls of the roll crusher:

1 – $\Delta = 3$ mm; 2 – $\Delta = 10$ mm

duction in a roll mill with a 2–3 mm roll gap is substantiated to prepare the material for fine classification and ensure optimal conditions for the maximum recovery of the titanomagnetite component in subsequent operations. Thus, at the ore-preparation stage for the inte-

grated utilization of tuff raw material, fine crushing in roll crushers, followed by reduction to a rational particle size, is sufficient to ensure the efficiency of subsequent dry magnetic separation [26].

The calculation of the technological performance indicators of dry magnetic separation of tuff for the initial material is presented in Table 1 (hereinafter referred to as Sample 1).

Based on the data presented in Table 1, the following features of sample crushing and subsequent magnetic separation can be highlighted:

1. Under the selected crushing scheme, the major portion of the tuff mass (63.8 %) is concentrated in the intermediate size class of $-1.6 + 0.25$ mm, whereas the remaining mass is distributed approximately equally between the coarse class $-2.5 + 1.6$ mm and the fine class -0.25 mm. This pattern of particle size distribution is consistent with the fact that tuff has a relatively low density $\rho \approx 1.3 \cdot 10^3$ kg/m³ and is characterized by high crushability.

2. In the considered narrow size classes, tuff demonstrates a pronounced tendency to separate into magnetic and non-magnetic fractions. For the total feed of -2.5 mm, the yield of the magnetic fraction is 54.6 %, whereas the yield of the non-magnetic fraction is 45.4 %. Thus, more than half of the mass of the initial raw material is recovered in the magnetic product, confirming the presence of a substantial magnetic-bearing component in the original material.

According to published sources, zeolite-smectite tuffs may contain about 49 % of a magnetic-bearing fraction by sample mass, with an iron content of 35–40 % and a titanium content of 2.5–4.0 %. This is consistent with the results obtained for the second sample.

The results of magnetic separation for another tuff sample (hereinafter referred to as Sample 2) are presented in Table 2. The calculations were performed based on experimental data.

As shown in Table 2 for particle size classes above 0.1 mm, more than 80 % of the material reports to the magnetic product, whereas the fine class, -0.1 mm, is non-magnetic and reports completely to the tailings.

Table 1

Results of dry magnetic separation of tuff (Sample 1)

Size class, mm	Feed yield, %	Magnetic fraction, %			Non-magnetic fraction, %		
		Yield	Grade	Recovery	Yield	Grade	Recovery
–2.5 + 1.6	17.2	9.9	0.20	33.5	7.3	0.007	4.4
–1.6 + 0.25	63.8	35.3	0.00	0.0	28.5	0.000	0.0
–0.25	19.0	9.4	0.10	21.0	9.6	0.050	41.0
Total	100.0	54.6	0.04	54.6	45.4	0.010	45.4

Table 2

Yield of magnetic separation products for tuff (Sample 2)

Size class, mm	Total in sample		Fraction, %				Yield from feed, %	
			Magnetic		Non-magnetic		Magnetic	Non-magnetic
	g	%	g	%	g	%	%	%
–2.5 + 0.63	331.4	36.1	275.0	83.0	56.4	17.0	29.94	6.14
–0.63 + 0.1	208.9	22.7	175.4	84.0	33.5	16.0	19.09	3.65
–0.1	378.3	41.2	0.0	0.0	378.3	100.0	0.00	41.18
Total	918.6	100.0	450.4	–	468.2	–	49.03	50.97

Results of the distribution function calculation

No	Induction (B), T	Product yield (y_i), g	Cumulative yield (y_z), g	Distribution function, (q_i), %
1	0.00	56.4	56.4	–
2	0.08	63.2	119.6	36.08
3	0.16	59.5	179.1	54.03
4	0.30	51.7	230.8	69.62
5	0.44	49.7	280.5	84.62
6	0.58	44.8	325.3	98.13
7	1.30	6.2	331.5	100.00

The overall product yield in Sample 2 is 49.03 % for the magnetic fraction and 50.97 % for the non-magnetic fraction. A comparison of the technological performance indicators for the two investigated samples shows that the product yield ratio (magnetic/non-magnetic) is 54.6/45.4 for Sample 1 and 49/51 for Sample 2. On average, for the two samples at a separator feed size of –2.5 mm, the magnetic fraction yield is 51.8 %.

Thus, the conducted studies confirm that tuff readily disintegrates during crushing and exhibits sufficient magnetic contrast for effective separation in a dry magnetic separator.

The magnetic properties of finely dispersed iron-bearing phases may vary substantially depending on the strength and frequency of the applied magnetic field [27]. To generalize the results, the most efficient narrow particle size classes for dry magnetic separation were investigated: +0.63–2.5 and +0.1–0.63 mm.

The analysis of dry magnetic separation results showed that the recovery of the magnetic-bearing fraction of tuff depends significantly on both magnetic field induction and particle size. For the coarser class (+0.63–2.5 mm), an increase in magnetic field induction is accompanied by a gradual decrease in the yield of the magnetic fraction: from maximum values at low inductions to a sharp reduction at high field strengths. In particular, the highest product portions are recovered at low induction levels (0.08–0.16 T), whereas a substantial decline in recovery is observed as the induction approaches 1.3 T.

For the finer class (+0.1–0.63 mm), the relationship is somewhat different: as induction increases to intermediate values, recovery rises, reaching a maximum at moderate magnetic field intensities (about 0.3 T), after which a gradual decrease is also observed. This behavior indicates that the finer fraction is more sensitive to changes in the magnetic field intensity and may require a narrower operating range for efficient separation.

At high magnetic field inductions, the recovery of the magnetic component becomes minimal for both size classes, indicating practically complete separation of the non-magnetic portion of the material. In addition, a considerable share of the material that does not respond to the magnetic field forms a separate non-magnetic fraction, which confirms the presence of a significant silicate component in the tuff raw material.

In the experiments, the tuff samples were represented by a 645 g batch, which included the investigated particle size classes and the silicate portion. The magnetic field induction was varied from 0 to 1.3 T. The obtained results reflect the distribution of material mass among portions recovered at different values of B , as well as the non-magnetic fraction; the correctness of the calculations is confirmed by the fact that the sum of the yields equals the mass of the corresponding size class.

Based on the initial experimental data, the distribution function of material recovery as a function of magnetic field induction was calculated. The distribution function q_i was defined as the fraction of the cumulative product yield up to the current induction value relative to the total mass of the investigated size class

$$q_i = \frac{y_i}{y_z} \cdot 100 \%,$$

where y_i is the yield of the magnetic product at a given induction; y_z is the total yield of the magnetic product in the sample.

The calculation results for the +0.63–2.5 mm size class are presented in Table 3.

The analysis of Table 3 shows that more than 98 % of the material is recovered at magnetic field inductions up to $B = 0.58$ T. In contrast, a further increase in induction to 1.3 T recovers less than 2 % of the remaining material. Thus, the dependence $q(B)$ exhibits a characteristic break point. Within the range up to 0.58 T, the cumulative yield increases intensively and relatively uniformly, after which the increment becomes sharply smaller. In view of the presence of this break point, the use of polynomial models for approximation is impractical, since they do not provide a physically adequate description over the entire interval. A linear-logarithmic relationship proved to be the most suitable for practical description, as it gives an adequate representation within the range of 0–0.9 T.

Optimizing analytical model parameters is a common task in the processing of geotechnical experimental data [28]. The analytical model of the distribution function was expressed in the form

$$q = a + b \cdot \ln(x), \quad (1)$$

where B is the magnetic field induction, T; q is the cumulative product yield, %; a , b are regression coefficients.

For the +0.63–2.5 mm size class, a regression model of form (1) was developed, for which the correlation coefficient was $P_z = 0.97$, the Fisher statistic was $F = 142.7$, and Student's t -statistics for the regression coefficients were $t_a = 44.14$ and $t_b = 11.95$

$$q_{+0.63-2.5} = 102.16 + 26.123 \cdot \ln(x).$$

For the +0.1–0.63 mm size class, a regression model of form (1) was similarly obtained, with a correlation coefficient of $P_z = 0.975$, the Fisher statistic of $F = 157.12$ and Student's t -statistics of $t_a = 42.15$ and $t_b = 12.53$

$$q_{+0.1-0.63} = 101.78 + 26.94 \cdot \ln(x).$$

The use of regression models to describe complex physicochemical systems is a widely applied approach in predicting phase composition and material properties [29]. The reported statistical indicators demonstrate strong correlation, high model adequacy, and significant regression coefficients [30]. Ensuring the stability and reproducibility of process parameters is a key element of quality and risk management in industrial technologies

Qualitative and quantitative elemental analysis of the magnetic fraction obtained from tuff beneficiation (XRF)

Chemical formula	Magnetic fraction, wt. %
Al ₂ O ₃	11.68
MgO	5.55
SiO ₂	40.15
K ₂ O	2.13
CaO	4.23
Cr ₂ O ₃	0.05
Ni ₂ O ₃	0.03
MnO ₂	0.69
Fe ₂ O ₃	30.89
CuO	0.02
ZnO	0.04
TiO ₂	4.23
V ₂ O ₅	0.23
Others	0.08

[31]. From a practical standpoint, it is important that the character of the $q(B)$ relationships for the two investigated size classes is uniform, which should be taken into account when substantiating DHIMS operating conditions in technological flowsheets for tuff processing. Similar approaches to describing separation processes in dispersed media using mathematical modeling have also been applied in the analysis of hydrodynamic processes for the recovery of valuable components [6].

The results of calculating the distribution function for tuff in the +0.63–2.5 mm size class, presented as experimental and calculated values of $q(B)$, are shown in Fig. 6.

As shown in Fig. 6 and the regression analysis results, the obtained models exhibit strong correlation, high approximation adequacy, and statistically significant regression coefficients. For practical applications, the acceptable magnetic field induction range is up to approximately $B \approx 0.9$ T, within which the model provides an adequate description of the experimental data. An important feature is the uniformity of the $q(B)$ relationships across the two investigated size classes, which should be taken into account when developing a technology for the integrated processing of tuff-bearing raw materials. Analytically, this is confirmed by the fact that the regression coefficients of the developed models fall within the same confidence interval at a significance level of ≤ 0.05 . Such modeling provides a basis for interpreting experimental data and for selecting rational operating parameters of dry high-intensity magnetic separation in industrial-scale processing schemes.

To confirm the qualitative characteristics of the magnetic fraction, a qualitative and quantitative elemental X-ray fluorescence (XRF) analysis was carried out using an Expert 3L rapid analyzer at Scientific and Manufacturing Company “PRODECOLOGIA”. The analysis made it possible to determine the elemental composition of the magnetic product and to assess the concentration of iron-bearing and associated components formed during the magnetic separation process. The results are presented in Table 4.

The obtained chemical composition of the magnetic fraction is promising for subsequent pyrometallurgical or electrothermal processing of concentrates [32]. According to Table 4, the magnetic fraction shows an elevated Fe₂O₃ content (30.89 %), consistent with the effective concentration of iron-bearing components in the magnetic product. At the same time, the magnetic frac-

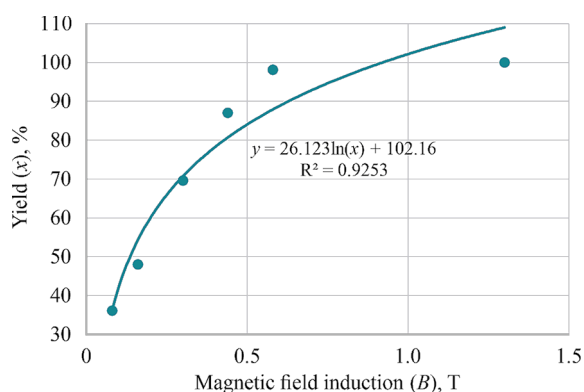


Fig. 6. Experimental and calculated values of the distribution function of tuff yield as a function of magnetic field induction for the +0.63–2.5 mm size class

tion also contains a substantial proportion of SiO₂ (40.15 %). This high value may be attributed to the presence of quartz and/or amorphous silica in the form of fine intergrowths or inclusions, as well as to the mechanical entrainment of the silicate component during separation [33], which is typical of finely dispersed systems and incomplete grain liberation [34].

The composition of the magnetic product indicates that it represents a complex iron-bearing concentrate containing both oxide and silicate phases. From a technological standpoint, this confirms that dry high-intensity magnetic separation primarily concentrates the titanomagnetite component while partially entraining the surrounding silicate matrix. Therefore, the efficiency of the process is strongly influenced by the degree of mineral grain liberation achieved during the crushing stage, which determines the selectivity of the subsequent magnetic separation.

Thus, the conducted studies confirm that tuff readily disintegrates during crushing and exhibits sufficient magnetic contrast for effective dry magnetic separation.

Further research should focus on determining the optimal combination of roll-crushing parameters and magnetic field induction for each narrow size class of tuff to maximize recovery of the titanomagnetite component at minimum energy consumption. Particular attention should be paid to the degree of mineral grain liberation after roll crushing, since incomplete liberation appears to be one of the main reasons for silica transfer into the magnetic product. It is also advisable to investigate the efficiency of multistage dry high-intensity magnetic separation for the +0.63–2.5 and +0.1–0.63 mm classes, as well as the processing potential of the fine fraction below 0.1 mm, which was found to report predominantly to the non-magnetic product. Another practically important direction is to assess the metallurgical suitability of the obtained magnetic fraction, particularly with respect to its Fe₂O₃, TiO₂ and SiO₂ contents, to substantiate possible routes for its further pyrometallurgical or electrothermal treatment.

Conclusions. The study examined the comminution characteristics of tuff. It confirmed its tendency toward intensive disintegration during crushing, which is important for achieving a rational particle-size distribution at the ore-preparation stage.

The presence of a magnetic-bearing component in the tuff was experimentally established, which substantiates the inclusion of dry high-intensity magnetic separation (DHIMS) in the technological flowsheet for the integrated processing of tuff raw material to separate the titanomagnetite (iron-bearing) fraction of the crushed mass.

Dry magnetic classification by narrow size classes showed that the most promising classes in terms of product yield and recovery of the magnetic-bearing fraction are +0.63–2.5 and +0.1–0.63 mm, which should be regarded as priority classes for industrial adjustment of DHIMS operating conditions.

The results were generalized in the form of experimental and regression relationships describing the variation in product yield/recovery as a function of separator magnetic field induction, which may be used to substantiate the operating induction range and to predict the technological performance of the process. It was established that more than 98 % of material recovery is achieved at magnetic field inductions up to $B=0.58$ T. In contrast, a further increase in induction provides only a minor additional gain in recovery.

The X-ray fluorescence elemental analysis of the magnetic fraction, performed using the Expert 3L rapid analyzer, showed an elevated Fe_2O_3 content (30.89 wt.%), which is consistent with the effective concentration of iron-bearing components in the magnetic product.

Acknowledgements. *The authors express their sincere gratitude to A. F. Bulat, Academician of the National Academy of Sciences of Ukraine and Director of the Institute of Geotechnical Mechanics, as well as to the research and production company Prodekoloziya for providing the opportunity to carry out the study using their laboratory facilities. The authors also thank the management of PJSC “Rafalivskiy Quarry”, represented by its Director P. P. Bortnyk, for enabling the sampling of tuff from the Rafalivskiy Quarry in the Rivne region, Ukraine.*

References.

1. Akhverdiev, A. T. (2024). To the problem of origin volcanoplutonic processes. *Mineral Resources of Ukraine*, (1), 59–63. <https://doi.org/10.31996/mru.2024.1.59-63>
2. Abdullayev, Z. B., Akhverdiev, A. T., Nagiyev, N. F., & Kerimova, T. E. (2023). The origin, conditions and mechanism for the formation of alpine-type hyperbasites of the Lesser Caucasus. *Mineral Resources of Ukraine*, (4), 48–55. <https://doi.org/10.31996/mru.2023.4.48-55>
3. Dychkovskiy, R., Saik, P., Sala, D., & Cabana, E. C. (2024). The current state of the non-ore mineral deposits mining in the concept of the Ukraine reconstruction in the post-war period. *Mineral Economics*. <https://doi.org/10.1007/s13563-024-00436-z>
4. Pavlychenko, A., & Kovalenko, A. (2013). The investigation of rock dumps influence to the levels of heavy metals contamination of soil. *Annual Scientific-Technical Collection – Mining of Mineral Deposits*, 237–238. <https://doi.org/10.1201/b16354-43>
5. Pavlychenko, A., Sala, D., Pyzalski, M., Dybrin, S., Antoniuk, O., & Dychkovskiy, R. (2025). Utilizing Fuel and Energy Sector Waste as Thermal Insulation Materials for Technical Building. *Energies*, 18(9), 2339. <https://doi.org/10.3390/en18092339>
6. Malanchuk, Z. R., Korniyenko, V. Y., Zaiets, V. V., Vasylchuk, O. Y., Kucheruk, M. O., & Semeniuk, V. V. (2023). Study of hydroerosion process parameters of zeolite-smectite tuffs and under-

- lying rock. *IOP Conference Series: Earth and Environmental Science*, 1254(1), 012051. <https://doi.org/10.1088/1755-1315/1254/1/012051>
7. Dychkovskiy, R., Dyczko, A., & Borojević Šošćarić, S. (2024). Foreword: Physical and Chemical Geotechnologies – Innovations in Mining and Energy. *E3S Web of Conferences*, 567, 00001. <https://doi.org/10.1051/e3sconf/202456700001>
 8. Buktukov, N., Gumennikov, Y., & Moldabayeva, G. (2024). Solutions to the Problems of Transition to Green Energy in Kazakhstan. *World-Systems Evolution and Global Futures*, 113–133. https://doi.org/10.1007/978-3-031-67583-6_6
 9. Kezembayeva, G., Rysbekov, K., Dyussenova, Z., Zhumagulov, A., Umbetaly, S., Barmenshinova, M., Yerkezhan, B., & Zhakypbek, Y. (2025). Public Health Risk Assessment of Quantitative Emission from a Molybdenum Production Plant: Case Study of Kazakhstan. *Engineered Science*, 34, 1454. <https://doi.org/10.30919/es1454>
 10. Dauletbaev, T. S., Mambetaliyeva, A. R., Dosmukhamedov, N. K., Zhandauletova, F. R., & Moldabaeva, G. Z. (2015). Complex Processing of Industrial Products and Lead-Copper Concentrates. *Eurasian Chemico-Technological Journal*, 17(4), 301–308. <https://doi.org/10.18321/ectj274>
 11. Malanchuk, Z., Zaiets, V., Tyhonchuk, L., Moshchych, S., Gayabazar, G., & Dang, P. T. (2021). Research of the properties of quarry tuff-stone for complex processing. *E3S Web of Conferences*, (280), 01003. <https://doi.org/10.1051/e3sconf/202128001003>
 12. Malanchuk, Y., Moshynskiy, V., Khrystyuk, A., Malanchuk, Z., & Korniyenko, V. (2025). Modeling the hydraulic washing-out process of amber-bearing rocks during amber extraction. *Mining of Mineral Deposits*, 19(2), 10–19. <https://doi.org/10.33271/mining19.02.010>
 13. Malanchuk, Z., Moshynskiy, V., Malanchuk, Ye., Korniyenko, V., Vasylchuk, O., Zaiets, V., & Kucheruk, M. (2023). Impact by the operating and structural parameters of a screen on the technological parameters of vibratory basalt sieving. *Mining of Mineral Deposits*, 17(2), 35–43. <https://doi.org/10.33271/mining17.02.035>
 14. Mamyrbayeva, K. K., Kuandykova, A. N., Chepushtanova, T. A., Merkiybayev, Y. S., & Brajendra, M. (2024). Studies of the extraction of nickel and cobalt from magnetic enrichment tailings. *Engineering Journal of Satbayev University*, 146(5), 1–9. <https://doi.org/10.51301/ejsu.2024.i5.01>
 15. Lozynskiy, V. (2023). Critical review of methods for intensifying the gas generation process in the reaction channel during underground coal gasification (UCG). *Mining of Mineral Deposits*, 17(3), 67–85. <https://doi.org/10.33271/mining17.03.067>
 16. Malanchuk, Y., Moshynskiy, V., Khrystyuk, A., Malanchuk, Z., Korniyenko, V., & Zhomyruk, R. (2024). Modelling mineral reserve assessment using discrete kriging methods. *Mining of Mineral Deposits*, 18(1), 89–98. <https://doi.org/10.33271/mining18.01.089>
 17. Fodor, M. M., Begentayev, M., & Turegeldinova, A. (2025). Supporting R,D&I in the creative industries. *Research, Development and Innovation in the Creative Industries*, 65, 65–78. Retrieved from <https://www.researchgate.net/publication/388693240>
 18. Abdurzakova, B. B., Kauanova, L. S., & Saimaganbetova, N. K. (2024). Analysis and research of flocculant reagents for thickening operations of flotation concentrate in the processing technology of fine-dispersed chrome ores. *Engineering Journal of Satbayev University*, 146(4), 16–23. <https://doi.org/10.51301/ejsu.2024.i4.03>
 19. Sarsembekov, T. K., Chepushtanova, T. A., & Merkiybayev, E. S. (2025). Economic analysis of the processing of various titanium-containing raw materials to obtain titanium, vanadium, and niobium. *Engineering Journal of Satbayev University*, 147(1), 1–7. <https://doi.org/10.51301/ejsu.2025.i1.01>
 20. Dakieva, K. Z., Tusupova, Z. B., Zhautikova, S. B., Loseva, I. V., Dzhangozina, D. N., Beysembaeva, R. S., & Zhamanbaeva, M. K. (2018). Studying the Benefits of Green Workplace Environment on Health Promotion in Sympathoadrenal and Kallikrein-Kinin Systems. *Ekoloji*, 27(106), 1087–1097.
 21. Khomenko, V., Pashchenko, O., Ratov, B., Koroviaka, Y., Kirin, R., & Tabylganov, M. (2025). Determination of the arrangement of electrodes for electrochemical fastening of borehole walls. *IOP Conference Series: Earth and Environmental Science*, 1481(1). <https://doi.org/10.1088/1755-1315/1481/1/012006>
 22. Dubovenko, Y. I., Nazirova, A. B., & Abdoldina, F. N. (2022). Data-driven preprocessing of gravity data in oilfield GIS monitoring system in Kazakhstan. *International Conference Monitoring of Geological Processes and Ecological Condition of the Environment*, (1), 1–4. <https://doi.org/10.3997/2214-4609.2022580267>
 23. Sailygarayeva, M., Nurlan, A., Rysbekov, K., Soltabayeva, S., Amralinova, B., & Baygurin, Z. (2023). Predicting of vertical displacements of structures of engineering buildings and facilities. *Nau-*

- koyvi Visnyk Natsionalnoho Hirnychoho Universytetu, (2), 77–83. <https://doi.org/10.33271/nvngu/2023-2/077>
24. Ismagulova, A. Z., Begentayev, M. M., & Tileuberdi, N. (2025). Studies of Influence of Lithological Composition of Overburden Rock on Colmation Process in Open-Type Infiltration Basins. *ES Materials and Manufacturing*, 28, 1473. <https://doi.org/10.30919/mmm1473>
25. Dairbekova, G., Zhautikov, B., Zobnin, N., Bekmagambetov, D., & Tolubayeva, D. (2021). Use of si-composite aspiration dusts production in the creation of thin-film anodes. *Metalurgija*, 60(3-4), 419–422.
26. Kalybekov, T., Rysbekov, K. B., Toktarov, A. A., & Otarbaev, O. M. (2019). Underground mine planning with regard to preparedness of mineral reserves. *Mining Informational and Analytical Bulletin*, (5), 34–43.
27. Berezniak, O., Mladetskiy, I., Berezniak, O., Dreshpak, O., & Akimov, O. (2025). High-frequency demagnetization of magnetite suspensions. *Mining of Mineral Deposits*, 19(2), 132–140. <https://doi.org/10.33271/mining19.02.132>
28. Nazirova, A., Kalimoldayev, M., Abdoldina, F., & Dubovenko, Y. (2022). Optimization of an information system module for solving a direct gravimetry problem using a genetic algorithm. *Eastern-European Journal of Enterprise Technologies*, 2 (9(116)), 21–34. <https://doi.org/10.15587/1729-4061.2022.253976>
29. Trembach, B., Hossain, M. M., Kabir, M. H., Silchenko, Y., Krbata, M., Sadovyi, K., Kolomitsev, O., & Ropyak, L. (2024). Prediction of Phase Composition and Mechanical Properties Fe–Cr–C–B–Ti–Cu Hardfacing Alloys: Modeling and Experimental Validations. *Heliyon*, 10(3), E25199. <https://doi.org/10.1016/j.heliyon.2024.e25199>
30. Aitkazanova, S., Soltabaeva, S., Kyrgyzbaeva, G., Rysbekov, K., & Nurpeisova, M. (2016). Methodology of assessment and prediction of critical condition of natural-technical systems. *International Multidisciplinary Scientific GeoConference Surveying Geology and Mining Ecology Management*, 2, 3–10. <https://doi.org/10.5593/sgem2016/b22/s09.001>
31. Efendiyev, G. M., Moldabayeva, G. Z., Buktukov, N. S., & Kuliyeu, M. Y. (2024). Comprehensive cementing quality assessment and risk management system. *SOCAR Proceedings*, (4), 42–47. <https://doi.org/10.5510/OGP20240401015>
32. Myrzakulov, M. K., Jumankulova, S. K., Barmenshinova, M. B., Martyushev, N. V., Skeebe, V. Y., Kondratiev, V. V., & Karlina, A. I. (2024). Thermodynamic and Technological Studies of the Electric Smelting of Satpaevsk Ilmenite Concentrates. *Metals*, 14(11), 1211. <https://doi.org/10.3390/met14111211>
33. Raimbekova, A., Kapralova, V., Popova, A., Kubekova, S., Dalbanbay, A., Kalenova, A., ..., & Myrzabekova, S. (2024). Corrosion behavior of mild steel in sodium sulfate solution in presence of phosphates of different composition. *Journal of Chemical Technology and Metallurgy*, 59(2), 367–377. <https://doi.org/10.59957/jctm.v59.i2.2024.16>
34. Yussupov, K., Abdissattar, G., Aben, E., Myrzakhmetov, S., Akhmetkanov, D., & Yelzhanov, E. (2025). A novel process for decolmatation of wells during in situ leach mining of uranium. *Civil Engineering Journal*, 11(4), 1447–1457. <https://doi.org/10.28991/CEJ-2025-011-04-011>

Моделювання процесу збагачення базальтового туфу шляхом сухої магнітної сепарації

З. Маланчук^{*1}, В. Мошинський¹, В. Лозинський²,
Є. Маланчук¹, В. Корнієнко³

1 – Національний університет водного господарства та природокористування, м. Рівне, Україна

2 – Національний технічний університет «Дніпровська політехніка», м. Дніпро, Україна

3 – Університет Коменського, м. Братислава, Словачька Республіка

* Автор-кореспондент e-mail: malanchykr@ukr.net

Мета. Встановити закономірності впливу індукції магнітного поля та гранулометричного складу на технологічні показники сухої високоінтенсивної магнітної сепарації (DHIMS) туфвої сировини та якість отриманого магнітного продукту.

Методика. Дослідження проведено на лабораторній установці сухої магнітної сепарації. Поведінку туфу вивчали у вузьких класах крупності +0,63–2,5 та +0,1–0,63 мм при зміні індукції магнітного поля в діапазоні 0–1,3 Тл за сталих конструктивних параметрів установки й режиму подачі матеріалу. Технологічні показники визначали за виходом магнітної й немагнітної фракцій, розрахунком функцій розподілу та побудовою регресійних моделей. Хімічний склад продуктів визначали методом рентгенофлуоресцентного аналізу.

Результати. Встановлено, що туф характеризується підвищеною магнітною сприйнятливостю й високою дробимістю, що створює передумови для ефективної сухої магнітної сепарації. Середній вихід магнітної фракції для двох досліджених проб становив 51,8 %, причому понад 98 % вилучення досягається при індукції магнітного поля до $B = 0,58$ Тл. Регресійні моделі демонструють високий ступінь кореляції ($P_z = 0,97–0,975$) у прийнятному діапазоні індукції до $B \approx 0,9$ Тл. Рентгенофлуоресцентний аналіз магнітного продукту показав вміст Fe_2O_3 – 30,89 %, що узгоджується із концентруванням залізовмісних компонентів у магнітній фракції.

Наукова новизна. Уперше виконано математичне моделювання процесу DHIMS туфу у вузьких класах крупності з визначенням функцій розподілу виходу продуктів магнітної сепарації залежно від індукції магнітного поля. Встановлені одноманітний характер залежностей для досліджених гранулометричних класів і статистична значущість параметрів регресійних моделей (рівень значущості $\leq 0,05$). Доведено, що лінійно-логіфічні моделі найкраще описують процес до індукції 0,9 Тл.

Практична значимість. Результати дозволяють обґрунтовано вибирати режими DHIMS для комплексної переробки туфів, визначати раціональні класи крупності для вилучення магнітно-вмісних домішок і прогнозувати ефективність процесу за значенням індукції магнітного поля. Отримані регресійні залежності можуть бути використані при проектуванні й оптимізації схем попереднього збагачення туфвої сировини з метою зменшення маси матеріалу, що надходить на подальші енергоємні операції.

Ключові слова: туф, суха магнітна сепарація, індукція магнітного поля, гранулометричний склад, залізовмісні мінерали, магнітна фракція

The manuscript was submitted 20.09.25.